Title

The same in the bulk but different as clusters: X3Y3 (X=B, Al, Ga; Y=P, As)

Authors

Alexandrova, Anastassia N
Nechay, Michael R
Lydon, Brian R
et al.

Publication Date

2013-11-01

DOI

10.1016/j.cplett.2013.10.003

Peer reviewed

Chemical Physics Letters 588 (2013) 37–42

Contents lists available at ScienceDirect

Chemical Physics Letters

journal homepage: www.elsevier.com/locate/cplett

The same in the bulk but different as clusters: X_3Y_3 (X = B, Al, Ga; Y = P, As)

Anastassia N. Alexandrova [a,b,*], Michael R. Nechay [a,1], Brian R. Lydon [a,1], Daniel P. Buchan [a,1], Alex J. Yeh [a,1], Ming-Hei Tai [a], Ivan P. Kostrikin [a], Lilit Gabrielyan [a]

[a] Department of Chemistry and Biochemistry, University of California, Los Angeles, Los Angeles, CA 90095-1569, United States
[b] California NanoSystems Institute, 570 Westwood Plaza, Building 114, Los Angeles, CA 90095, United States

ARTICLE INFO

Article history:
Received 29 August 2013
In final form 1 October 2013
Available online 9 October 2013

ABSTRACT

Most binary materials formed by early group 13 and 15 elements are semiconductors identical in their structures and properties. We show that in the ultra-small cluster regime these materials are markedly different. Among X_3Y_3 (X = B, Al, Ga; Y = P, As), lighter clusters are planar, and heavier clusters are compact and three-dimensional. The difference is owed to the interplay between covalency and delocalized non-directional bonding in these systems. If the sp-hybridization in the constituent elements is energetically affordable and leads to strong directional overlap, the bonding is covalent and the cluster is flat. Otherwise, the cluster is three-dimensional.

1. Introduction

Miniaturization of functional units in material science opens vast opportunities for applications, ranging from catalysis, to medicine, to optical materials. Undoubtedly, at the tiny scale, matter looks and behaves differently due to electronic effects such as quantum confinement (in the nanoparticle regime), or completely different molecular-like chemical bonding phenomena (in sub-nano clusters). Here, we study binary clusters formed by groups 13 and 15 elements. In the bulk, binary mixtures of group 13 and group 15 atoms are semiconductors and have interesting electrical properties, such as GaAs which is used in solar panels [1] or GaP which has seen use in various LED devices [2]. These mixtures are valence isoelectronic with carbon, and most of them form zinc blende structures in the bulk [3], though some more exotic crystal structures are known [4]. The indirect band gaps of these materials range from 1.4 to 2.5 eV [5]. At the smaller scale, these materials are used as quantum dots of characteristic different colors in the visible range of the electromagnetic spectrum. Quantum dots are especially desirable for their uses in LEDs and biological fluorescence imaging. There have been some syntheses of small (~1 nm) quantum dots, with GaAs particles of 5.1 nm average size and GaP particles of 2.3 nm average size [6]. These kinds of compounds would be desirable in a practical sense, as they will allow the expansion of previous applications to lower wavelengths or higher energy applications. Notice that all discussed quantum dots have the crystal structures of the bulk material, and the differences between those formed by any combination of B, Al, Ga and P, As, Sb are very subtle.

In this work, we investigate these binary materials at the sub-nano scale, in the cluster regime. The considered X_3Y_3 (X = B, Al, Ga; Y = P, As) binary clusters have not been studied before. Surprisingly, unlike their virtually identical bulk analogues, these tiny clusters are found to differ dramatically in their shapes and electronic characteristics, as will be shown. Some difference in fact could be anticipated, based on the subtle differences in electronegativities of the constituent elements and varying extents of the valence atomic orbitals (AOs) available for bonding. Some of the studied clusters appear to be flat or two-dimensional (2-D), and some are three-dimensional (3-D). We will discuss the found differences on the basis of the chemical bonding within these clusters, and identify the origin of the effect as being in the degree of affordable covalency of chemical bonding. It is important that the found effect is not observable at the larger scale and is characteristic only of the sub-nano regime.

2. Theoretical methods

An automated extensive search for the global minima was performed for all discussed clusters. The searches were done with our in-house *ab initio* Gradient Embedded Genetic Algorithm (GEGA) [7–9] program at the B3LYP [10–12]/3-21G [13,14] level of theory. Separate searches were performed for singlets and triplets. For every structure of every spin state, three independent runs of the GEGA search were performed. Details of the algorithm can be found elsewhere [7–9]. The population size in GEGA was 30,

* Corresponding author at: Department of Chemistry and Biochemistry, University of California, Los Angeles, Los Angeles, CA 90095-1569, United States.
E-mail address: ana@chem.ucla.edu (A.N. Alexandrova).
[1] These authors equally contributed to this work.

0009-2614/$ - see front matter © 2013 Elsevier B.V. All rights reserved.
http://dx.doi.org/10.1016/j.cplett.2013.10.003

and the convergence was considered sufficient when the current most stable structure was the same for 20 consecutive iterations. From our experience, GEGA performs exceptionally well for finding the global minima of clusters, as was confirmed in numerous joint theoretical and experimental spectroscopic studies [7–9,15–27]. The lowest energy isomers found to be within 20 kcal/mol from the global minimum were retained for further consideration. Their geometries and vibrational frequencies were refined at the B3LYP/6-311 + G*, and MP2 [28,29]/6-311 + G* levels of theory. Additionally, single point energies were calculated using CCSD(T) [30–36]/6-311 + G(2df)//MP2/6-311 + G*. The analysis of chemical bonding was done with NBO [37–41] at the B3LYP/6-311 + G* level, and MO analysis at the HF/6-311 + G* level. Finally, single point energy calculations at CASSCF(n,m) [42–48]/6-311 + G* (n = 4–6, m = 4–6) were carried out for the MP2 geometries, in order to check the validity of the single determinant methods. It was confirmed that all considered species have unequivocally single configuration wave functions, and hence, the single reference methods are considered reliable. GAUSSIAN 09 [49] was used for all calculations.

3. Results and discussion

3.1. Structures

For each of the studied clusters, X_3Y_3 (X = B, Al, Ga; Y = P, As), the found the global minimum and two additional lowest energy isomers are shown in Figure 1. These species were found using the GEGA algorithm and refined at higher levels of theory. The calculated molecular properties of these, as well as other isomers are presented in the Supporting Information (SI). Most of the lowest energy species appeared to be singlets, with B_3As_3 being a noticeable exception (triplet in the global minimum state). Notice the radical differences between the global minima of the clusters formed by lighter elements and those formed by heavier elements. Both clusters containing B are flat (B_3P_3 and B_3As_3). Also, all isomers of the B-containing clusters, and not just the global minima, contain a B_3 triangular unit. This robust unit was identified as the main building block of all pure-B clusters [50], and also mixed B–C [25] and B–Al clusters [20]. B_3 is covalently bound, containing three 2 center – 2 electron B–B bonds. The B–B bonds in B_3P_3 and B_3As_3 are 2.14 Å (1.71 Å in the triplet) and 1.70 Å, respectively, i.e., longer than those found in the pure B_3^- cluster (1.54 Å). Al forms an identical flat cluster when bound to P, but not to As. The Al–Al distance in the isolated Al_3^- triangular cluster is 2.58 Å, and it is also elongated in Al_3P_3 (2.89 Å). Al_3As_3 is 3-D. Finally, both clusters of Ga are 3-D, and their structures are analogous to that of Al_3As_3, containing the P_3 or Ga_3 triangle at the base of the capped bipyramid.

3.2. Chemical bonding

It is remarkable that the global minima of the studied clusters do not look the same, and we would like to understand the origin of this difference. For this, we analyzed the chemical bonding in the studied clusters using MO and NBO analyses. For all 2-D and 3-D structures, MOs look very similar, and thus we focus only on one representative species of each structural class. Valence MOs are shown in Figure 2.

Let us focus on the 2-D clusters first. In Table 1 we collect the calculated natural atomic charges and other bonding characteristics of the flat clusters. NBO analysis on the 2-D structure, taking B_3As_3 as our representative cluster, shows that there are six covalent B-As σ-bonds along the periphery of the cluster. Those σ-bonds are formed by sp-hybridized atoms of B and As. Hybridization is typical for B, whose 2s- and 2p-AOs are close in energy.

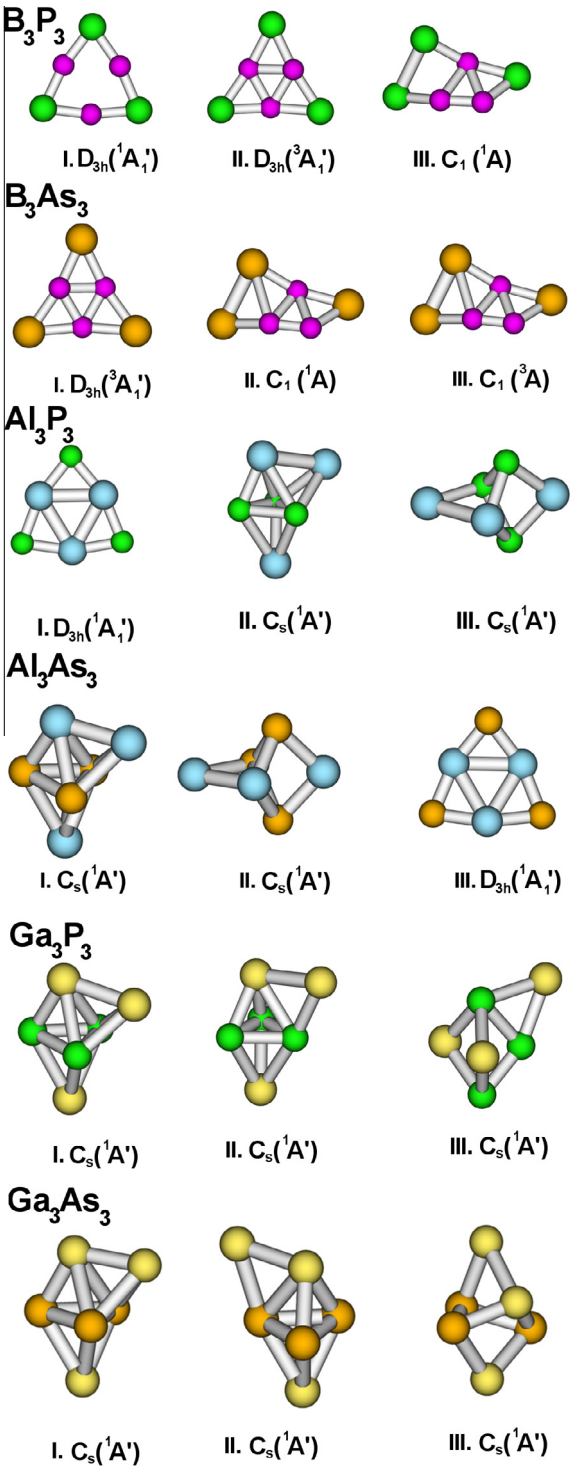

Figure 1. Global and lowest-energy local minima of the studied clusters systems, as found by GEGA. Relative energies given are calculated at the CCSD(T)/6-311 + G(2df) level of theory. Magenta – B, green – P, blue – Al, orange – As, yellow – Ga. (For interpretation of the references to colour in this figure legend, the reader is referred to the web version of this article.)

It is, however, surprising to see AOs of As also mix significantly (see Table 1 for the s- and p-contributions to the localized covalent bonds from the B and As atoms). Other flat clusters also exhibit these covalent bonds, whose formation is facilitated by AO-mixing (Table 1). MOs that are localizable as 2c–2e bonds in a typical 2-D cluster are outlined in grey in Figure 2A.

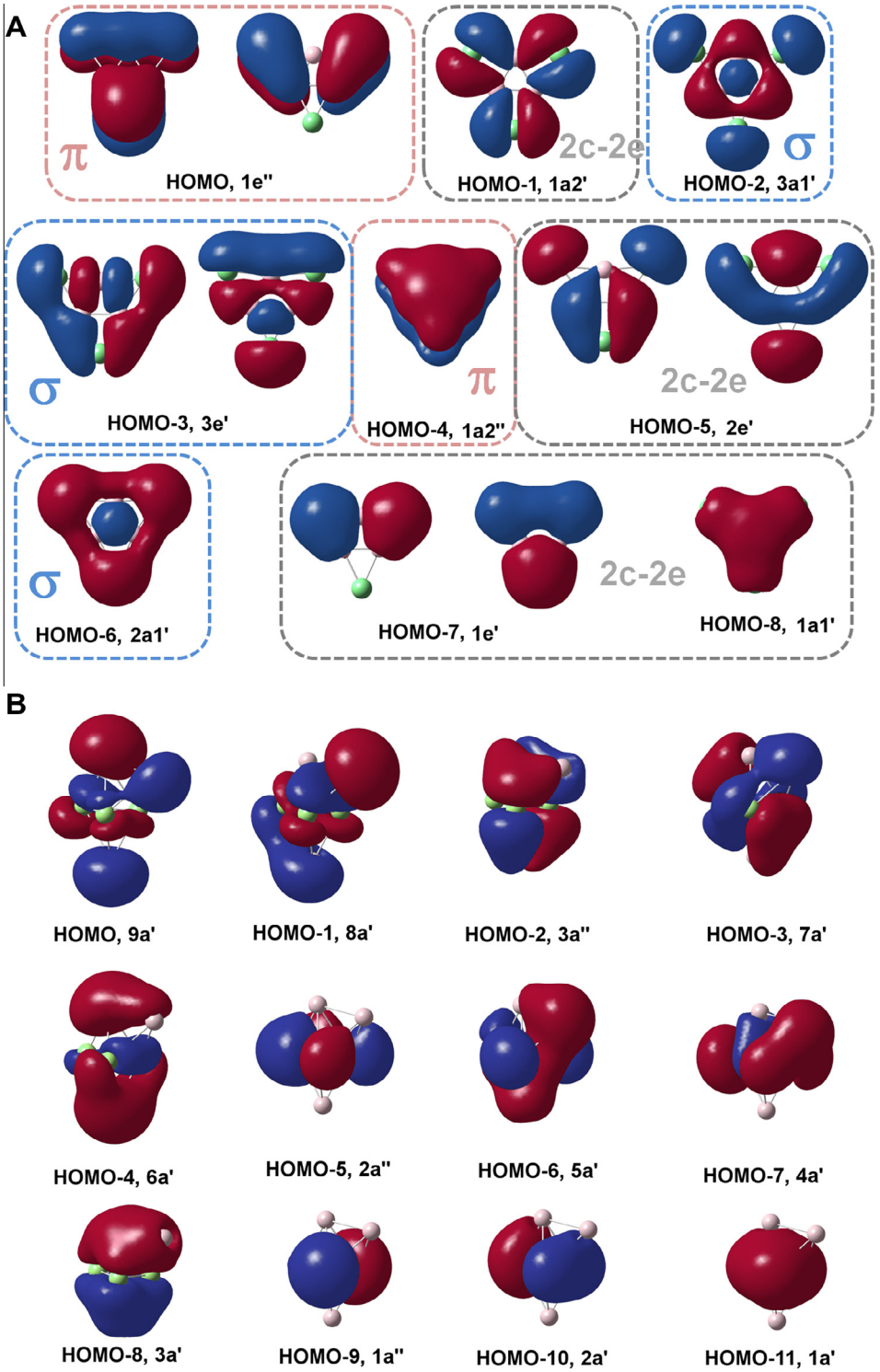

Figure 2. Valence MOs of B_3As_3 (A) and Al_3As_3 (B), representative of all 2-D and 3-D clusters in the studied group, respectively. For the 2-D cluster, MOs characteristic of the triplet state are shown. The difference between it and the singlet state is discussed in the text.

The rest of the electron density in the cluster is delocalized. It is easy to spot three π-MOs: one completely bonding (HOMO-4), and a degenerate pair of partially bonding HOMOs populated by two electrons in the triplet state. Occupied by a total of four electrons, these MOs make the triplet 2-D clusters obey the $(4n)$ Hückel's rule for aromatic open-shell compounds, and therefore, this cluster is π-aromatic. The singlet ground state clusters of B_3P_3 and Al_3As_3 have this degenerate π-set populated by four electrons, making the systems obey the regular $(4n + 2)$ rule for aromatic systems. Of the MOs shown in Figure 2A, it is the HOMO-2 that gets unpopulated in the singlet state.

There are also delocalized σ-MOs: the completely bonding HOMO-6, the partially bonding degenerate pair, HOMO-3, and the HOMO-2. The HOMO-2 is an interesting MO of the radial type in which the contributions from B and As are in antiphase and so it is antibonding between As and B, but bonding within the B_3 cycle.

Table 1
Composition of localized MOs corresponding to the classical 2 center – 2 electron σ-bonds in the planar clusters, showing the degree of sp-hybridization, and natural charges on atoms in the global minimum structures (results of NBO analysis at the B3LYP/6-311 + G* level of theory). X = B, Al; Y = P, As.

	B_3P_3	B_3As_3	Al_3P_3
sp-mixing on *X*	49% s + 51% p	29% s + 71% p	50% s + 50% p
sp-mixing on *Y*	19% s + 81% p	11% s + 89% p	10% s + 90% p
Q(*X*)	−0.05	−0.44	+0.89
Q(*Y*)	+0.05	+0.44	−0.89
e-Negativity(*Y*) – e-Negativity(*X*)	0.15	0.14	0.58

This MO is responsible for the additional contraction of the B_3-triangle in the triplet state. It is unoccupied in all 2-D singlets. To confirm that for singlets it is indeed the true ground state, we performed additional tests, where we swapped the $1a_2'$ HOMO-2 with the $3a_1'$ LUMO and optimized this species; it appeared to be 41 kcal/mol above the ground state at the B3LYP/6-311 + G* level. Another possible state is the singlet with the degenerate HOMO populated by two antiferromagnetically coupled electrons; however, it would be picked by the CASSCF calculations, and it was not. Therefore, the reported state is the true ground state. The four radial σ-MOs are formed by the sp-hybrids pointing into the cycle. These hybrids are orthogonal to those responsible for covalent bonding in the system. Radial σ-bonding bonds all six atoms, but involves only four electron pairs, and in this sense is 'electron-deficient', i.e. these MOs cannot be localized as 2c–2e classical bonds. The radial σ-bonding is delocalized. The singlet clusters obey the $(4n + 2)$ rule for σ-aromatic compounds. For the triplet state, strictly speaking, σ-MOs do not make the system obey the traditional Hückel's rules. However, these MOs are not localizable and do not break the symmetry of the cluster. It is therefore legitimate to call the triplet system σ-aromatic. Hence, in addition to strong covalent bonding, the 2-D clusters are doubly-aromatic, π- and σ-. Aromaticity is a characteristic of delocalized bonding, and delocalized bonding is optimal in 3-D, where delocalized overlap can be maximized. Therefore, it is covalency that is responsible for flattening the system. This flattening effect of covalency on cluster structure has been observed previously in other cluster systems [20–22].

If one were to compare B_3As_3, B_3P_3, and Al_3As_3, the covalent σ-bonding within them is the same, and facilitated by the AO-hybridization of the same quality (Table 1). It is in many ways surprising to see this uniformity. For example, a comparison between B_3P_3 and Al_3P_3 presents a curious case. It was previously shown that B and Al differ majorly in their ability to undergo sp-hybridization: B is highly likely to do it, whereas Al is more reluctant due to the greater energy-separation of its 3s- and 3p-AOs. This difference manifests itself in distinctly different shapes of B and Al clusters [20].

However, by binding to P in the planar clusters, Al undergoes sp-mixing of AOs to the same degree as B does. However, the 3-D isomer of Al_3P_3 is very close in energy (Figure 1). Notice that Ga is unable to bind in a 2-D way to P, while it is more electronegative than Al (1.81 vs. 1.61) and closer in electronegativity to P (2.19). This has to do with AO energies and sizes, and the lack of possible efficient overlap between AOs of large Ga and much smaller P.

Notice also the degrees of charge-transfer (CT) in the systems (Table 1). In Al_3P_3, the CT is most pronounced and correlates with the difference in electronegativities of Al and As. However, for B_3P_3 and B_3As_3 the trend is not explainable by a simple electronegativity argument. The triplet B_3As_3 cluster is a CT species, with B_3 being effectively negatively charged, and pulling electron density from As in order to facilitate the intra-B-cycle binding.

Now let us turn attention to the 3-D clusters, Al_3As_3, Ga_3P_3, and Ga_3As_3. Figure 2B contains valence MOs characteristic of all these 3-D structures. According to the NBO analysis, the bases of the capped bipyramids are covalently bound As_3 and P_3 units: there are three σ-bonds formed by sp-hybrids on the three atoms (Table 2). These localized MOs are populated by ca. 1.94 electrons. AO-mixing is also reflected in the natural electronic configurations of atoms, for example the P atoms in Ga_3P_3 have the following configuration: $[Ne]3s^{1.76}3p^{3.69}$, i.e., the 3s-population is significantly depleted to the expense of AO-mixing. Al/Ga do not undergo AO-mixing; these atoms' s-AOs remain populated by close to 2 electrons for all 3-D clusters. Each of the MOs shown in Figure 2B contains contributions coming from either primarily s-AOs or primarily p-AOs on Al/Ga. Thus, Al/Ga do not bind to the base of the bipyramid covalently. Instead, the rest of the electron density is delocalized throughout the cluster. Delocalized overlap is most extensive in 3-D rather than in 2-D. Hence, the globular 3-D shapes are explained on the basis of the lack of covalent bonding between the P_3/As_3 unit and 3Al/3 Ga atoms. Therefore, we witness another case where covalency and delocalized bonding drive cluster structures toward completely different shapes [20–22], and appear to oppose each other in defining them. Thus, covalency and delocalized bonding are levers of cluster design.

Qualitatively, it is clear that the degree of AO-hybridization, responsible for the change of cluster shapes, is governed by the atom's own electronic structure (in this case the energy separation of the valence s- and p-AOs), and the quality of the covalent overlap with the partner atom or group of atoms that can be achieved due to this mixing. In Table 3, we present the calculated parameters related to this qualitative description: ε_s and ε_p are calculated energies of the occupied valence s- and p-AOs in atoms (HF/6-311 + G*); $\varepsilon_{s-p-\text{average}}$ are the averaged energies of s- and p-AOs, qualitatively reflecting the energetic 'center' of the valence shell; $\Delta\varepsilon_{s-p-\text{average}}$ are the differences between these quantities for the pair of elements constituting the corresponding binary cluster; and [E(3-D)-E(2-D)] are energy differences between the lowest energy 3-D isomer (structure analogous to that of the global minimum of Al_3As_3, Figure 1) and the 2-D isomer (structure analogous to that of the global minimum of Al_3P_3, Figure 1). For some of the systems, the prototypical 2-D or 3-D isomers do not exist, and for them, the difference in energy is not reported in Table 3. For the three systems that have both 2-D and 3-D isomers, we plotted the correlation between [E(3-D)-E(2-D)] and the simple sum of the parameters that we deduce to be responsible for the degree of AO-mixing: $(\varepsilon_p - \varepsilon_s)_X + (\varepsilon_p - \varepsilon_s)_Y + \Delta\varepsilon_{s-p-\text{average}}$ (Figure 3). The former two terms correlate with the elements' internal 'willingness' to mix s- and p-AOs, and the latter term correlates with the 'willingness' to mix s- and p-AOs in response to bonding with the particular partner atom. Even though the number of data points in Figure 3 is small, the nearly perfect linear correlation is educational, and suggests that our analysis of the impact of AO-mixing on structure is correct.

Table 2
Composition of localized MOs corresponding to the classical 2 center – 2 electron σ-bonds in the 3-D clusters, showing the degree of sp-hybridization, and natural charges on atoms in the global minimum structures (results of NBO analysis at the B3LYP/6-311 + G* level of theory). X = Al, Ga; Y = P, As.

	Al_3As_3	Ga_3P_3	Ga_3As_3
sp-mixing on *Y*	5% s + 95% p	8% s + 92% p	5% s + 95% p
$Q(X)_{\text{average}}$	+0.46	+0.43	+0.41
$Q(Y)_{\text{average}}$	−0.46	−0.43	−0.41
e-Negativity(*Y*) – e-Negativity(*X*)	0.57	0.38	0.37

Table 3
Relevant AO energy differences in a.u., calculated at HF/6-311 + G*, and corresponding energy differences between the 3-D and 2-D isomers calculated at B3LYP/6-311 + G*, in a.u. Pink cells correspond to 2-D clusters, and blue cells correspond to 3-D clusters.

	B: $\varepsilon_p - \varepsilon_s = 0.23$ $\varepsilon_{s-p-\text{average}} = -0.43$	Al: $\varepsilon_p - \varepsilon_s = 0.21$ $\varepsilon_{s-p-\text{average}} = -0.32$	Ga: $\varepsilon_p - \varepsilon_s = 0.24$ $\varepsilon_{s-p-\text{average}} = -0.33$
P: $\varepsilon_p - \varepsilon_s = 0.41$ $\varepsilon_{s-p-\text{average}} = -0.56$	$\Delta\varepsilon_{s-p-\text{average}} = 0.13$ E(3-D)-E(2-D) – n/a	$\Delta\varepsilon_{s-p-\text{average}} = 0.24$ E(3-D)-E(2-D) = 0.0117	$\Delta\varepsilon_{s-p-\text{average}} = 0.23$ E(3-D)-E(2-D) = 0.0197
As: $\varepsilon_p - \varepsilon_s = 0.41$ $\varepsilon_{s-p-\text{average}} = -0.54$	$\Delta\varepsilon_{s-p-\text{average}} = 0.11$ E(3-D)-E(2-D) – n/a	$\Delta\varepsilon_{s-p-\text{average}} = 0.22$ E(3-D)-E(2-D) = −0.00187	$\Delta\varepsilon_{s-p-\text{average}} = 0.21$ E(3-D)-E(2-D) – n/a

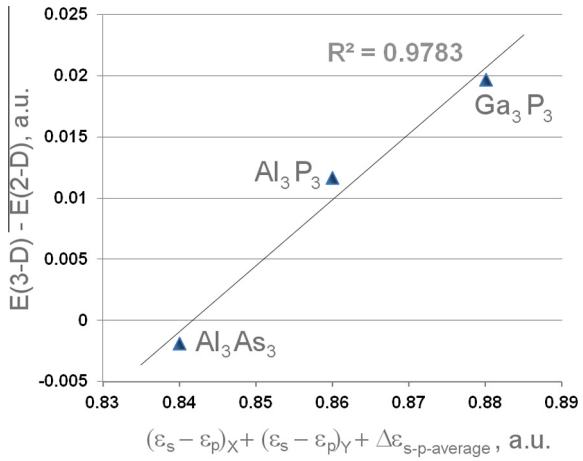

Figure 3. Observed qualitative linear relation between the difference in the total energies of the planar (covalent) and 3-D (non-covalent) structures and the simple empirical function that is a sum of the s-p separation in the elements constituting the clusters (X = B, Al, Ga; Y = P, As) and the energy difference between the 'middle' of the valence shells of X and Y. The former two terms correlate with the elements' internal 'willingness' to mix s- and p-AOs, and the latter term correlates with the 'willingness' to mix s- and p-AOs in response to bonding with the particular partner atom.

4. Conclusions

We showed that, in striking contrast to uniform structures in the bulk, binary clusters formed by the elements of groups 13 and 15 are different in shape and bonding. B_3P_3, B_3As_3, and Al_3P_3 are planar species, possessing six classical 2–c–2e bonds between constituent elements, and double aromaticity (σ- and π-) in 2-D. On the other hand, Al_3As_3, Ga_3P_3, and Ga_3As_3 are globular capped bipyramidal structures. In them, only the P_3/As_3 unit at the base of the pyramid is covalently bound, and the rest of bonding is delocalized over the entire cluster. We show that the difference in shapes is due to the degree of AO-mixing or hybridization attained in constituent elements. Hybridization is driven by the energy-proximity of s- and p-AOs to mix, and by the quality of the covalent overlap with the neighboring atom that can be achieved due to this mixing, as qualitatively demonstrated in Table 3 and Figure 3. This is another example of covalency and delocalized bonding opposing each other in defining cluster shapes. Covalency drives the clusters flat, compromising delocalized bonding in 2-D, whereas delocalized bonding is optimal in most globular shapes, and those are promoted by delocalized overlap. The two bonding effects thus constitute two levers of cluster design.

Acknowledgment

This work was supported by the ACS PRF grant 51052-NDI6 to ANA.

Appendix A. Supplementary data

Supplementary data associated with this article can be found, in the online version, at http://dx.doi.org/10.1016/j.cplett.2013.10.003.

References

[1] Nobel Lecture by Zhores Alferov, p. 6.
[2] K. Lohnert, E. Kubalek, Phys. Status Solidi. 80 (1983) 173.
[3] G.L.W. Hart, A. Zunger, Phys. Rev. B 62 (2000) 13522.
[4] H. Chen, G. Wang, M. Dudley, Z. Xu, J.H. Edgar, T. Batten, M. Kuball, L. Zhang, Appl. Phys. Lett. 92 (2008) 231917.
[5] O. Madelung, Semiconductors: Data Handbook, Springer-Verlag, Berlin, Heidelberg, 2004.
[6] J.F. Janik, R.L. Wells, V.G. Young, A.L. Rheingold, I.A. Guzei, J. Am. Chem. Soc. 120 (1998) 532.
[7] A.N. Alexandrova, J. Phys. Chem. A 114 (2010) 12591.
[8] A.N. Alexandrova, A.I. Boldyrev, J. Chem. Theory Comput. 1 (2005) 566.
[9] A.N. Alexandrova, A.I. Boldyrev, Y.-J. Fu, X. Yang, X.-B. Wang, L.S. Wang, J. Chem. Phys. 121 (2004) 5709.
[10] R.G. Parr, W. Yang, Density-Functional Theory of Atoms and Molecules, Oxford Univ. Press, Oxford, 1989.
[11] A.D. Becke, J. Chem. Phys. 98 (1993) 5648.
[12] J.P. Perdew, J.A. Chevary, S.H. Vosko, K.A. Jackson, M.R. Pederson, D.J. Singh, C. Fiolhais, Phys. Rev. B 46 (1992) 6671.
[13] T. Clark, J. Chandrasekhar, C.W. Spitznagel, P.V.R. Schleyer, J. Comput. Chem. 4 (1983) 294.
[14] M.J. Frisch, J.A. Pople, J.S. Binkley, J. Chem. Phys. 80 (1984) 3265.
[15] A.N. Alexandrova, A.L. Boldyrev, X. Li, H.W. Sarkas, J.H. Hendricks, S.T. Arnold, K.H. Bowen, J. Chem. Phys. 134 (2011) 044322–044328.
[16] A.N. Alexandrova, A.I. Boldyrev, H.-J. Zhai, L.-S. Wang, J. Phys. Chem. A 109 (2005) 562.
[17] D.Yu. Zubarev, A.N. Alexandrova, A.I. Boldyrev, L.-F. Cui, X. Li, L.-S. Wang, J. Chem. Phys. 124 (2006) 124305.
[18] A.N. Alexandrova, K.A. Birch, A.I. Boldyrev, J. Am. Chem. Soc. 125 (2003) 10786.
[19] J.C. Bopp, A.N. Alexandrova, B.M. Elliott, T. Herden, M.A. Johnson, Int. J. Mass Spectrom. 283 (2009) 94.
[20] M. Huynh, A.N. Alexandrova, J. Phys. Chem. Lett. 2 (2011) 2046.
[21] A.N. Alexandrova, Chem. Phys. Lett. 533 (2012) 1.
[22] A.N. Alexandrova, M.J. Nayhouse, M.T. Huynh, J.L. Kuo, A.V. Melkonian, G. Chavez, J. De, N.M. Hernando, M.D. Kowal, C.-P. Liu, Phys. Chem. Chem. Phys. 14 (2012) 14815.
[23] L.F. Cui, X. Huang, L.-M. Wang, D.Yu. Zubarev, A.I. Boldyrev, J. Li, L.S. Wang, J. Am. Chem. Soc. 128 (2006) 8390.
[24] L.-M. Wang, W. Huang, L.S. Wang, B.B. Averkiev, A.I. Boldyrev, J. Chem. Phys. 130 (2009) 134303–134307.
[25] B.B. Averkiev, D. Zubarev, J. Am. Chem. Soc. 130 (2008) 9248.
[26] W. Tiznado, N. Perez-Peralta, R. Islas, A. Toro-Labbe, J.M. Ugalde, G. Merino, J. Am. Chem. Soc. 131 (2009) 9426.
[27] C. Ortega-Moo, J. Cervantes, M.A. Mendez-Rojas, K.H. Pannell, G. Merino, Chem. Phys. Lett. 490 (2010) 1.
[28] M. Head-Gordon, J.A. Pople, M.J. Frisch, Chem. Phys. Lett. 153 (1988) 503.
[29] M.J. Frisch, M. Head-Gordon, J.A. Pople, Chem. Phys. Lett. 166 (1990) 275.
[30] M.J. Frisch, M. Head-Gordon, J.A. Pople, Chem. Phys. Lett. 166 (1990) 281.
[31] J. Cizek, Adv. Chem. Phys. 14 (1969) 35.
[32] G.D. Purvis III, R.J.A. Bartlett, J. Chem. Phys. 76 (1982) 1910.
[33] G.E. Scuseria, C.L. Janssen, H.F. Schaefer III, J. Chem. Phys. 89 (1988) 7382.
[34] G.E. Scuseria, H.F. Schaefer III, J. Chem. Phys. 90 (1989) 3700.
[35] J.A. Pople, M. Head-Gordon, K.J.A. Raghavachari, J. Chem. Phys. 87 (1987) 5968.
[36] P.J. Knowles, C. Hampel, H.-J. Werner, J. Chem. Phys. 99 (1993) 5219.
[37] J.E. Carpenter, F. Weinhold, J. Mol. Struct. (THEOCHEM) 169 (1988) 41.
[38] Carpenter, J. E. Ph.D. Thesis, University of Wisconsin, Madison, WI, 1987.
[39] J.P. Foster, F. Weinhold, J. Am. Chem. Soc. 102 (1980) 7211.
[40] A.E. Reed, F. Weinhold, J. Chem. Phys. 78 (1983) 4066.
[41] A.E. Reed, L.A. Curtiss, F. Weinhold, Chem. Rev. 88 (1988) 899.

[42] K. Raghavachari, G.W. Trucks, J.A. Pople, M. Head-Gordon, Chem. Phys. Lett. 157 (1989) 479.
[43] D. Hegarty, M.A. Robb, Mol. Phys. 38 (1979) 1795.
[44] R.H.A. Eade, M.A. Robb, Chem. Phys. Lett. 83 (1981) 362.
[45] H.B. Schlegel, M.A. Robb, Chem. Phys. Lett. 93 (1982) 43.
[46] F. Bernardi, A. Bottini, J.J.W. McDougall, M.A. Robb, H.B. Schlegel, Faraday Symp. Chem. Soc. 19 (1984) 137.
[47] M.J. Frisch, I.N. Ragazos, M.A. Robb, H.B. Schlegel, Chem. Phys. Lett. 189 (1992) 524.
[48] N. Yamamoto, T. Vreven, M.A. Robb, M.J. Frisch, H.B. Schlegel, Chem. Phys. Lett. 250 (1996) 373.
[49] M.J. Frisch, G.W. Trucks, H.B. Schlegel, G.E. Scuseria, M.A. Robb, J.R. Cheeseman, G. Scalmani, V. Barone, B. Mennucci, G.A. Petersson, H. Nakatsuji, M. Caricato, X. Li, H.P. Hratchian, A.F. Izmaylov, J. Bloino, G. Zheng, J.L. Sonnenberg, M. Hada, M. Ehara, K. Toyota, R. Fukuda, J. Hasegawa, M. Ishida, T. Nakajima, Y. Honda, O. Kitao, H. Nakai, T. Vreven, J.A. Montgomery Jr., J.E. Peralta, F. Ogliaro, M. Bearpark, J.J. Heyd, E. Brothers, K.N. Kudin, V.N. Staroverov, R. Kobayashi, J. Normand, K. Raghavachari, A. Rendell, J.C. Burant, S.S. Iyengar, J. Tomasi, M. Cossi, N. Rega, N.J. Millam, M. Klene, J.E. Knox, J.B. Cross, V. Bakken, C. Adamo, J. Jaramillo, R. Gomperts, R.E. Stratmann, O. Yazyev, A.J. Austin, R. Cammi, C. Pomelli, J.W. Ochterski, R.L. Martin, K. Morokuma, V.G. Zakrzewski, G.A. Voth, P. Salvador, J.J. Dannenberg, S. Dapprich, A.D. Daniels, Ö. Farkas, J.B. Foresman, J.V. Ortiz, J. Cioslowski, D.J. Fox, GAUSSIAN 09, Revision A.1, Gaussian Inc., Wallingford CT, 2009.
[50] A.N. Alexandrova, A.I. Boldyrev, H.-J. Zhai, L.-S. Wang, Coord. Chem. Rev. 250 (2006) 2811.